

## Research Paper

PAIN®

OPEN

# Brain perfusion patterns are altered in chronic knee pain: a spatial covariance analysis of arterial spin labelling MRI

Sarina J. Iwabuchi<sup>a,b,c</sup>, Yue Xing<sup>b,c</sup>, William J. Cottam<sup>a,b,c</sup>, Marianne M. Drabek<sup>a,b,c</sup>, Arman Tadjibaev<sup>a,b,c</sup>, Gwen S. Fernandes<sup>a,d</sup>, Kristian K. Petersen<sup>e,f</sup>, Lars Arendt-Nielsen<sup>e,f</sup>, Thomas Graven-Nielsen<sup>f</sup>, Ana M. Valdes<sup>a,b,d</sup>, Weiya Zhang<sup>a,b,d</sup>, Michael Doherty<sup>a,b,d</sup>, David Walsh<sup>a,b,d</sup>, Dorothee P. Auer<sup>a,b,c,\*</sup>

## Abstract

Chronic musculoskeletal pain is a common problem globally. Current evidence suggests that maladapted central pain pathways are associated with pain chronicity, for example, in postoperative pain after knee replacement. Other factors such as low mood, anxiety, and tendency to catastrophize are also important contributors. We aimed to investigate brain imaging features that underpin pain chronicity based on multivariate pattern analysis of cerebral blood flow (CBF), as a marker of maladaptive brain changes. This was achieved by identifying CBF patterns that discriminate chronic pain from pain-free conditions and by exploring their explanatory power for factors thought to drive pain chronification. In 44 chronic knee pain and 29 pain-free participants, we acquired both CBF and T1-weighted data. Participants completed questionnaires related to affective processes and pressure and cuff algometry to assess pain sensitization. Two factor scores were extracted from these scores representing negative affect and pain sensitization. A spatial covariance principal component analysis of CBF identified 5 components that significantly discriminated chronic pain participants from controls, with the unified network achieving 0.83 discriminatory accuracy (area under the curve). In chronic knee pain, significant patterns of relative hypoperfusion were evident in anterior default-mode and salience network hubs, while hyperperfusion was seen in posterior default mode, thalamus, and sensory regions. One component correlated positively with the pain sensitization score ( $r = 0.43$ ,  $P = 0.006$ ), suggesting that this CBF pattern reflects neural activity changes encoding pain sensitization. Here, we report a distinct chronic knee pain-related representation of CBF, pointing toward a brain signature underpinning central aspects of pain sensitization.

**Keywords:** Chronic pain, ASL, Cerebral blood flow, PCA, Knee osteoarthritis, MRI, Experimental pain, Sensitization

## 1. Introduction

Chronic musculoskeletal (MSK) pain is a common public health, social, and economic problem<sup>36</sup> with prevalence rates between 20% and 44% in the United Kingdom and United States.<sup>12,14</sup>

*Sponsorships or competing interests that may be relevant to content are disclosed at the end of this article.*

<sup>a</sup> Versus Arthritis Pain Centre, University of Nottingham, Nottingham, United Kingdom, <sup>b</sup> NIHR Nottingham Biomedical Research Centre, Queen's Medical Centre, University of Nottingham, Nottingham, United Kingdom, <sup>c</sup> Sir Peter Mansfield Imaging Centre, School of Medicine, University of Nottingham, Nottingham, United Kingdom, <sup>d</sup> Division of Rheumatology, Orthopaedics and Dermatology, School of Medicine, University of Nottingham, Nottingham City Hospital, Nottingham, United Kingdom, <sup>e</sup> SMI, Department of Health Science and Technology, Faculty of Medicine, Aalborg University, Aalborg, Denmark, <sup>f</sup> Center for Neuroplasticity and Pain (CNAP), SMI, Faculty of Medicine, Aalborg University, Aalborg, Denmark

\*Corresponding author. Address: Radiological Sciences, Room W/B 1441, Queen's Medical Centre, Nottingham NG7 2UH, United Kingdom. Tel.: +44 (0)115 823 1178. E-mail address: Dorothee.Auer@nottingham.ac.uk (D.P. Auer).

Supplemental digital content is available for this article. Direct URL citations appear in the printed text and are provided in the HTML and PDF versions of this article on the journal's Web site ([www.painjournalonline.com](http://www.painjournalonline.com)).

PAIN 161 (2020) 1255–1263

Copyright © 2020 The Author(s). Published by Wolters Kluwer Health, Inc. on behalf of the International Association for the Study of Pain. This is an open access article distributed under the Creative Commons Attribution License 4.0 (CCBY), which permits unrestricted use, distribution, and reproduction in any medium, provided the original work is properly cited.

<http://dx.doi.org/10.1097/j.pain.0000000000001829>

Unfortunately, as many as 40% of people living with chronic pain report unsatisfactory effect of treatment,<sup>8</sup> highlighting a clear and urgent need to better understand chronic pain mechanisms for developing better treatments.

Recent work has focused on identifying specific neural signatures to explain the varied processes that contribute to the experience of physical pain,<sup>45</sup> but relatively little progress has been made to unravel the neural basis of the chronic pain experience. Cerebral blood flow (CBF) as measured using arterial spin labeling (ASL) is particularly well-suited to study chronic pain because it allows the capture of an absolute measure of nonevoked brain activity that underlies a “tonic” state such as ongoing spontaneous pain. To date, few CBF studies have investigated chronic pain, with even fewer studies in MSK pain.<sup>11,21,24,46,47</sup> Observations of CBF changes in chronic MSK pain<sup>21,46,47</sup> are not consistent and are often limited by small sample sizes ( $N \leq 17$ ), although appear to show a pattern of widespread hyperperfusion. Increased CBF in osteoarthritis has been observed in premotor, somatosensory, salience network regions, thalamus, amygdala, hippocampus and midbrain regions (including the periaqueductal gray) that were related to ongoing pain.<sup>21</sup> Similarly, Wasan et al.<sup>47</sup> reported increased CBF in similar cortical regions as well as hyperperfusion in an area of the dorsal attention network during worsening of clinical pain in chronic low back pain. One recent study using a slightly larger sample ( $N = 26$ ) did not observe any CBF differences between osteoarthritis (OA) participants and healthy

controls, although did observe an association between ongoing pain and regional CBF in areas predominantly involved in emotional and fear regulation.<sup>11</sup> Most of these studies use either voxel-wise or region-of-interest methods, which are known to lack the sensitivity to capture effects that may be more subtle and spatially distributed.

Multivariate analysis of CBF data provides a data-driven way to extract latent features of ongoing coordinated brain activity even from multiple parallel processes. This approach may allow for the decoding of these processes and determine which markers distinguish participants with chronic pain from those without pain; a similar approach has been applied to distinguish subjects with and without Parkinson's disease.<sup>31</sup> Recently, a Gaussian process classifier was applied to CBF data to discriminate presurgical and postsurgical molar extraction intervention with just under 95% accuracy,<sup>33</sup> demonstrating that certain CBF features are associated with acute severe pain in a clinical setting. To extend this further toward clinically relevant chronic pain, we aimed to identify novel discriminating markers of chronic pain in a population of largely community-dwelling people with mild–moderate knee pain and explore how these features relate to specific facets of the chronic pain experience.

The purposes of this study were to use a multivariate approach (principal components analysis) to (1) discriminate participants with chronic knee pain from pain-free controls using nonevoked brain activity measures and (2) determine whether these differences in CBF covariance patterns are related to affective or sensitized pain mechanisms in the pain syndrome. We hypothesized that the discriminatory components would comprise previously reported regions of CBF changes somatosensory, salience, and dorsal attentional network regions; the thalamus, amygdala, and hippocampus; and key regions of the descending and ascending pain modulatory pathways, notably the periaqueductal gray. In addition, we hypothesized that these CBF patterns would differentially correlate with pain sensitization and affective pain phenotypes.

## 2. Materials and methods

### 2.1. Design and participants

This was a cross-sectional nested study within a larger knee OA multidimensional phenotyping study (INCOPE, Imaging Neural Correlates of Osteoarthritis Phenotypes) that will be reported in a future manuscript. For this CBF substudy, the initial batch of the full INCOPE data set comprising 54 participants with chronic knee pain and 33 healthy and pain-free participants was included (from a total data set of 87 chronic knee pain participants and 39 healthy and pain-free participants), allowing for a reasonably matched group of chronic knee pain and pain-free controls to test our multivariate approach on CBF data. The relationship between sample size and discriminatory accuracy and hence power is complex for multivariate pattern analysis or machine-learning approaches because increasing sample heterogeneity may more than offset gains from larger sample sizes.<sup>38</sup> The final sample of 78 participants compares favourably with the bulk of published ASL brain imaging studies and multivariate pattern analysis studies to discriminate complex psychiatric disorders.<sup>23</sup> The larger chronic knee pain cohort also allowed for regression analyses within the group. Recruitment pathways were from a database of participants from the community through the East Midlands–based Knee Pain and Related Health in the Community study cohort (Nottingham Research Ethics Committee 1, NREC reference 14/EM/0015; registered with ClinicalTrials.gov [NCT02098070])<sup>15,16</sup> (N = 53),

primary care through general practitioner surgeries (N = 27) within the Nottinghamshire region, or secondary care through the Sherwood Forest Hospitals NHS Foundation Trust orthopaedic referrals or poster advertisements at Nottingham City Hospital (N = 7). All participants completed a set of questionnaires, quantitative sensory testing (QST), followed by an MRI session. The study was approved by the Nottingham Research Ethics Committee 2 (NREC reference: 10/H0408/115), and all participants provided written informed consent. Inclusion criteria for chronic knee pain participants was self-reported diagnosis of knee osteoarthritis and/or reported chronic pain in the knee (ie, pain for most of the day and pain for >14 days/month), and their knee pain was their most troublesome pain. Healthy participants reported no current or past history of knee pain (nor pain elsewhere). Participants were excluded if they had any history of stroke or had any current major neurological condition, psychosis, or had a contraindication to MRI (full list of inclusion and exclusion criteria is provided in the supplementary materials, available at <http://links.lww.com/PAIN/A966>).

### 2.2. Psychometric data

Participants all underwent psychometric assessments before the MRI scan session. Pain intensity on the day was taken in the hour before scanning using a numerical rating scale ranging from 0 (no pain) to 100 (worst imaginable pain). Questionnaires included the Beck's Depression Inventory II<sup>6</sup> (BDI-II), the Trait Anxiety Scale of the State-Trait Anxiety Inventory (STAI-T)<sup>42</sup> and the Pain Catastrophizing Scale (PCS),<sup>43</sup> which was broken down into the subscales of helplessness, magnification, and rumination. The BDI-II and the STAI-T were converted using Rasch conversion following the method of Lincoln et al.,<sup>28</sup> which recommended the BDI-II to be divided into 2 subscales (negative thoughts and negative behaviours) for measuring depression in participants with osteoarthritis.

### 2.3. Quantitative sensory testing

All participants underwent QST before the MRI scan session, which consisted of pressure algometry (pressure pain thresholds [PPTs]) using a handheld pressure algometer with a 1-cm<sup>2</sup> probe, and pressure was increased at a rate of approximately 30 kPa/s (Somedic AB, Sösdala, Sweden), and cuff pressure algometry using a computer-controlled cuff algometer (Cortex Technology and Aalborg University, Denmark). The pressure algometry assessed PPTs at 2 sites: the sternum and the most painful knee (or either knee in pain-free healthy controls). The cuff pressure algometry assessed pressure pain detection threshold (PDT), pressure pain tolerance threshold (PTT), temporal summation of pain (TS), and conditioned pain modulation (CPM) using the same method as described in previous studies.<sup>35,37,44</sup> Detailed methods of the QST is provided in the supplementary materials (available at <http://links.lww.com/PAIN/A966>).

### 2.4. MRI data acquisition

Participants underwent multimodal MRI at 3T (Discovery MR750; GE Healthcare, Chicago, IL) using a 32-channel head coil, as part of a larger phenotyping study (INCOPE) including ASL data and T1-weighted anatomical data used for image registration, which are reported here for the CBF pattern substudy. Cerebral blood flow was assessed using a pulsed-continuous ASL sequence with 3D spiral read-out (tag/control image pairs = 72, flip angle = 111°, TE = 10.536 ms, TR = 4844 ms, labelling duration = 1450 ms,

postlabelling duration = 2025 ms, field of view = 240 mm, slice thickness = 4 mm, slice gap = 4 mm, number of slices = 36, echo train length = 1, number of excitations = 3, matrix =  $128 \times 128$ , and voxel resolution =  $1.875 \times 1.875 \times 4$  mm).<sup>13</sup> Arterial spin labeling imaging also used background suppression and an  $M_0$  image for image quantification in line with current recommendations.<sup>2</sup> High-resolution anatomical images were acquired in the sagittal plane using a fast-spoiled gradient echo sequence (TE/TR = 3.164/8.132 ms, T1 = 450 ms, slice gap = 1 mm, field of view = 256, matrix =  $256 \times 256$ , flip angle =  $12^\circ$ , and voxel resolution = 1 mm<sup>3</sup>). T1-weighted images were acquired parallel to the AC-PC line, while the bottom of the acquired ASL image was positioned just below the cerebellum to allow for whole-brain CBF imaging.

## 2.5. Image preprocessing

Each image was visually assessed for quality including artefacts induced by motion and poor labelling defined by extremely low CBF values in the occipital regions ( $<20$  mL/100 g/min) relative to the rest of the cortex. Following quality control, there were 10 chronic knee pain and 4 healthy control data sets excluded from the final analysis resulting in a total of 44 chronic knee pain and 29 healthy and pain-free control subjects. Cerebral blood flow maps (mL/100 g/min) were produced with the use of an automatic reconstruction script as reported in Zaharchuk et al.<sup>48</sup> Both the T1-weighted images and CBF maps were first skull-stripped using the brain extraction tool from FSL v5.0.11 (FMRIB Software Library). The CBF maps were then linearly registered to the T1-weighted images and then to MNI space using FLIRT v6.0 (FMRIB's Linear Image Registration Tool).<sup>22</sup> The images were then spatially smoothed using a 5-mm full-width half-maximum Gaussian kernel and masked to exclude voxels that had a probability of less than 42% gray matter. This was chosen as it provided the most reliable CBF measures in an independent test-retest data set (unpublished). These masked images were then used in the principal component analysis (PCA) analysis.

## 2.6. Principal components analysis of cerebral blood flow data

A voxel-based principal components analysis was used to generate patterns of spatial covariance in gray matter perfusion across the sample. We followed the method of Spetsieris et al.<sup>41</sup> and Melzer et al.<sup>31</sup> whereby the data were log-transformed and demeaned using the subject's mean perfusion and the group mean and then entered in a principal component analysis to calculate the eigenvectors and eigenvalues of the covariance. The spatial images of principal components with unit variance were generated using the same approach as it was proposed previously.<sup>31</sup> As a result, the first 16 components were selected, which explained 87.8% of the variance, with the first component captured the most variance and the last component accounts for the least. A backward stepwise binomial logistic regression was used to determine the components, which successfully distinguished pain participants and pain-free controls (based on Akaike Information Criterion). These components were then linearly combined to create a unified network representing a chronic knee pain-related perfusion network and z-scores. To test for the network reliability, a 500 permutation bootstrap estimation method was employed using the same approach as Melzer et al.<sup>31</sup>

## 2.7. Region of interest analysis

To validate the PCA findings, we also applied a region-of-interest analysis to determine whether the patterns of hyperperfusion and

hypoperfusion were reflected in absolute CBF changes. The positive and negative loadings (thresholded at  $z > 1.96$  and  $z < -1.96$ , respectively) and the remaining regions of the unified network and component 12 (the one component of 16 correlating with QST factor score) were masked onto each subject's CBF map to extract mean CBF values. Age, sex, and mean global CBF were regressed out of the absolute CBF data, and all subsequent analyses were applied to the residuals. For the behavioural measures, both age and sex were regressed out of the data. Mean CBF of the unified network and component 12 were then compared between the 2 groups. In addition, the component 12 positive and negative loading CBF means for chronic knee pain participants were correlated with the QST factor score to explore whether the relationship was driven by hyperperfusion or hypoperfusion.

## 2.8. Statistical analyses

We performed the Kaiser–Meyer–Olkin test and Bartlett's test of sphericity to ensure that a factor analysis was suitable for dimension reduction of both the psychometric and QST scores. This dimension reduction approach allows for the integration of numerous variables gathered from psychometric questionnaire scores and QST scores to provide measures reflecting an overall measure of negative affect and sensitization respectively. Unrotated principal components analysis was used to extract a principal component for the psychometric scales and the QST scores using SPSS v25.0.0.1.

To address our primary outcome, a binomial generalised linear model was used to predict the labels of participants with chronic knee pain and healthy controls using each CBF component alone as well as the unified network, and the area under the receiver-operating characteristic curve (AUC) was analysed to assess the performance of the prediction. The AUC was obtained using Matlab 2018a for all the individual components and the unified network.

For the second outcome, we used the PCA-derived pain sensitization and affect scores to relate to CBF measures. Linear regression was used to relate the network scores of the chronic knee pain group with numerical rating scale pain severity score, affect factor score and QST factor score, correcting for age and sex. For the region-of-interest analyses of absolute CBF, age, sex, and mean global CBF were regressed out of the data, and all subsequent analyses were applied to the residuals. Mean global CBF was also compared between groups after regressing out age and sex. For the behavioural measures, both age and sex were regressed out of the data. Mean CBF comparisons between groups was performed using an independent-sample *t* test. All analyses used an  $\alpha$  level of  $P < 0.05$ .

## 2.9. Data availability

Anonymised data may be made available upon request to the authors.

## 3. Results

Demographics, psychometric, and QST results in the final cohort of chronic knee pain participants and controls are provided in **Table 1**. Table of medications are included in the supplementary materials (available at <http://links.lww.com/PAIN/A966>).

### 3.1. Psychometric data

Between-group comparisons showed significant differences for BDI-II–negative behaviour subscale, PCS, and all PCS subscales (**Table 1**). The Kaiser–Meyer–Olkin measure (0.81) and significant Bartlett's test of sphericity ( $P < 0.0001$ ) indicated that a factor

**Table 1****Demographic and clinical data of participants.**

Data	Knee pain participants	Healthy controls	P
N	44	29	—
Mean age	62.82 (8.63)	64.41 (11.07)	0.49
Sex (male/female)	22/22	18/11	0.31
Laterality of affected knee (L/R)	22/22	—	—
Mean educational scores	5*	3*	<b>0.02</b>
Pain duration (mo)	119.68 (121.94)	—	—
NRS pain 0–100 on the d	36.3 (29.35)*	—	—
PainDETECT (Rasch converted)	−0.58 (0.72)*	—	—
BDI-II negative thoughts subscale (Rasch converted)	2.85 (3.04)	1.7 (2.16)	0.07
BDI-II negative behaviours subscale (Rasch converted)	9.41 (3.25)	5.25 (3.2)	<b>&lt;0.001</b>
STAI-T (Rasch converted)	−1.32 (1.51)	−1.77 (0.93)	0.124
PCS	18.37 (14.43)*	9.17 (7.44)	<b>&lt;0.01</b>
PCS: helplessness	8.53 (6.32)*	3.21 (3.11)	<b>&lt;0.01</b>
PCS: magnification	3.35 (3.44)*	1.9 (1.57)	<b>0.04</b>
PCS: rumination	6.81 (5.17)*	4.07 (3.58)	<b>0.02</b>
PPT sternum [kPa]	260.5 (162.32)*	300.43 (161.68)*	0.31
PPT knee [kPa]	308.72 (202.47)*	398.94 (221.5)*	0.08
PDT affected leg [kPa]	17.48 (6.81)*	21.28 (7.99)†	<b>0.04</b>
PTT affected leg [kPa]	32.9 (13.27)*	39.4 (14.8)†	0.06
PDT unaffected leg [kPa]	17.24 (6.91)*	19.63 (9.37)‡	0.23
PTT unaffected leg [kPa]	30.55 (12.07)*	35.74 (13.86)‡	0.11
TS [VAS points]	0.99 (1.25)†	0.6 (0.95)†	0.16
CPM [kPa]	4.83 (8.36)†	9.49 (10.27)‡	<b>0.04</b>
Affect factor score	0.31 (1.12)*	−0.46 (0.54)	<b>0.001</b>
QST factor score	0.04 (1)†	0.59 (1.02)‡	<b>0.03</b>

Values displayed are mean values and SDs (in parentheses). Education is scored as 1 with highest level of qualification to 8 with no formal education. PainDETECT Rasch conversion according to Lincoln et al. (2017). Bold indicates significant group differences (uncorrected for multiple comparisons).

\* One subject score missing.

† Two subject scores missing.

‡ Three subject scores missing.

BDI-II, Beck's depression index; CPM, conditioned pain modulation; NRS, numerical rating scale; PCS, Pain Catastrophizing Scale; PPT, pressure pain threshold; PDT, pain detection threshold; PTL, pain tolerance threshold; STAI-T, State-Trait Anxiety Inventory; TS, temporal summation; QST, quantitative sensory testing.

analysis was suitable for dimension reduction of the BDI-II subscales, STAI-T, and the PCS subscale scores. The extracted principal component explained 68.7% of the variance. This component loaded positively on all scores with maximum loading for PCS helplessness, where higher factor scores indicated more negative affective characteristics (**Table 2**).

### 3.2. Quantitative sensory testing data

Between-group comparisons revealed a significantly lower PDT of the affected leg and reduced CPM in chronic pain participants (**Table 1**). There was also a trend toward greater sensitivity in chronic knee pain participants for the PPT of the knee and PTT of the affected leg ( $P < 0.1$ , **Table 1**). A total of 8 scores were derived from the QST (PPT of sternum and knee, PDT and PTT of each leg, TS, and CPM). The Kaiser-Meyer-Olkin test (0.65) and Bartlett's test of sphericity ( $P < 0.0001$ ) indicated suitability of a factor analysis for dimension reduction of the QST scores. The

extracted component explained 54.5% of the total variance which loaded positively and highly on all measures indicating greater pain sensitivity (maximum ipsilateral (PTT) except for the TS, where high scores indicate greater sensitivity resulting in negative loading albeit of much smaller extent (**Table 3**).

**Table 2****Component loading scores for the affective measures.**

Affect measures	Component 1
Trait anxiety (STAI-T)	0.81
PCS helplessness	0.91
PCS magnification	0.87
PCS rumination	0.83
BDI-II negative thoughts	0.80
BDI-II negative behaviours	0.75

BDI, Beck's depression index; PCS, Pain Catastrophizing Scale; STAI-T, State-Trait Anxiety Inventory.



**Table 3**  
**Component loading scores for the QST measures.**

QST measures	Component 1
PPT sternum	0.77
PPT knee	0.68
TS	−0.16
CPM	0.75
PDT affected leg	0.82
PTT affected leg	0.89
PDT unaffected leg	0.77
PTT unaffected leg	0.81

CPM, conditioned pain modulation; PPT, pressure pain threshold; PDT, pain detection threshold; PTT, pain tolerance threshold; TS, temporal summation; QST, quantitative sensory testing.

### 3.3. Principal components of cerebral blood flow data

The PCA extracted 16 components that were used for predicting group classification. Components 2, 6, 8, 12, and 13 significantly classified knee pain participants from controls. These components explained 19.9%, 2.2%, 1.3%, 1%, and 0.9% of the variance, respectively, and were considered to be knee pain-related components. The AUC of the unified network was 0.83 while the 5 included individual components yielded 0.62 to 0.64 classification power. The unified network achieved 82% specificity and 76% sensitivity. The unified component and component 12 are illustrated in **Figures 1A and B**, respectively, with details of cluster regions (clusters >20 voxels) listed in **Table 4**.

Of the 5 discriminatory components, only component 12 was significantly associated with the QST factor score ( $r = 0.43$ ,  $P = 0.006$ ). The affect factor score was not significantly correlated with any of the knee pain-related components. Correlation between the discriminating components and the individual QST and affect measures can be found in the supplementary materials (available at <http://links.lww.com/PAIN/A966>). Pain severity did not significantly correlate with any of the 5 discriminatory components. Of note, flipping the images of those in the knee pain cohort with a painful left knee to test the effect of pain laterality did not significantly alter the ability for the combined component to discriminate between healthy and knee pain participants (data not shown).

### 3.4. Region-of-interest analysis

#### 3.4.1. Unified network

Mean CBF (ml/100g/min) was significantly higher in participants with knee pain ( $M = 50.23$ ,  $SEM = 0.48$ ) compared with healthy controls ( $M = 47.01$ ,  $SEM = 0.54$ ) within the knee pain-related perfusion network with positive loadings ( $t(71) = 4.38$ ,  $P < 0.001$ , **Fig. 1C**), and significantly lower CBF (knee pain participants:  $M = 47.93$ ,  $SEM = 0.43$ ; pain-free controls:  $M = 50.49$ ,  $SEM = 0.43$ ) was seen within the regions with negative loadings ( $t(71) = -4.02$ ,  $P < 0.001$ , **Fig. 1C**), confirming that the positive and negative loadings reflect hyperperfusion and hypoperfusion, respectively. Conversely, mean CBF outside of the pain-related network (ie, gray matter regions that did not reach the threshold for positive or negative loadings) did not differ between chronic knee pain and pain-free participants (knee pain participants:  $M = 48.94$ ,  $SEM = 0.02$ ; pain-free controls:  $M = 48.97$ ,  $SEM = 0.02$ ).

#### 3.4.2. Component 12

Clusters from component 12 with positive and negative factor loading showed significant hyperperfusion ( $t(71) = 3.26$ ,  $P = 0.002$ ) and

hypoperfusion ( $t(71) = -2.36$ ,  $P = 0.02$ ) in pain participants vs controls. Within the chronic knee pain group, absolute CBF averaged over the networks of component 12 showed a significant positive association with the QST factor for the positive regions ( $r = 0.423$ ,  $P = 0.005$ ) but no significant association for the negative regions ( $r = -0.224$ , *ns*). These results are illustrated in **Figure 1D**. A closer inspection of this CBF correlation was performed to explore the correlation with individual QST measures, which showed an association with all measures except for TS (these results are provided in the supplementary materials, available at <http://links.lww.com/PAIN/A966>).

Mean global CBF did not differ significantly between both groups ( $P = 0.72$ ). In addition, as the chronic pain signature did not include the periaqueductal gray (PAG) as expected,<sup>9,19,22</sup> we undertook a regional periaqueductal gray (PAG) post hoc analysis to mitigate against the risk that the PCA dimensionality reduction may fail to detect small clusters forming local networks. As shown in the supplementary results (available at <http://links.lww.com/PAIN/A966>), mean PAG CBF suggested hyperperfusion in chronic knee pain participants compared with controls.

## 4. Discussion

Using PCA of CBF data, we have identified a novel covariance pattern derived from nonevoked brain activity that discriminates chronic knee pain participants from pain-free controls. This discriminating knee pain-related network revealed a pattern of hypoperfusion/hyperperfusion within extended pain connectome regions. A component of the hyperperfusion network was related to the degree of pain sensitization pointing to a brain signature underpinning the central aspects of pain sensitization.

### 4.1. Knee pain-related network and its link to sensitisation measures

The ability of CBF covariance maps to clearly discriminate between chronic pain and pain-free groups and highlights the dual advantage of combining a multivariate pattern approach with a quantitative physiological measure of brain activity as previously exploited for acute pain.<sup>33</sup> There is, however, evidence demonstrating spatial correlation between network hubs measured through fMRI and CBF<sup>27</sup> allowing for comparisons across modalities, albeit with caution. The knee pain-related network corresponds well with regions considered part of the pain connectome from resting-state fMRI, with a distinct pattern of increased perfusion in posterior default mode network (DMN) regions and reduced perfusion in salience network regions. Previous studies commonly report dysfunctions of regions comprising both the DMN and salience network in various chronic pain conditions and across a range of imaging modalities.<sup>3,4,9,21,26,30</sup> In one study using CBF data to discriminate presurgical and postsurgical third molar extraction, the multivariate pattern of perfusion classifying postsurgical painful state<sup>33</sup> is in striking contrast to the current unified component classifying chronic knee pain participants. They showed increased CBF after surgery in the thalamus, salience network, secondary somatosensory, and anterior cingulate cortices, with decreased CBF in visual and parietal cortices. This dissociative pattern between our knee pain participants with mild ongoing pain and the postsurgery participants with severe acute pain from O'Muircheartaigh et al.'s study, thus largely excludes upregulated nociception as underlying mechanism, and conversely suggests a maladaptive neuroplasticity process linked to pain chronification.

The observed CBF pattern of chronic pain showed, however, an overlap with the acute postsurgical pain CBF signature

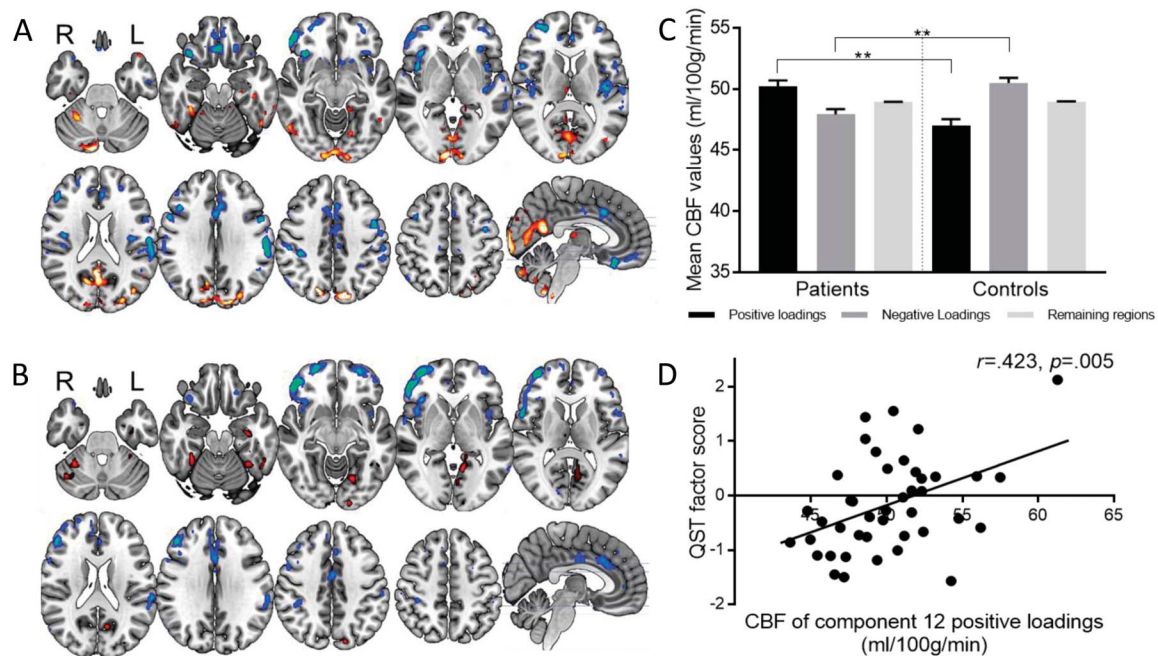


**Figure 1.** Components discriminating people with chronic pain and healthy controls and their association with pain sensitization. (A) The unified knee pain-related network (combination of 5 components) that classified chronic knee pain participants and controls. Clusters in hot colours are regions with positive loadings, clusters in cold colours are regions with negative loadings. (B) Component 12 from the PCA that classified chronic knee pain participants from controls. This component was also significantly correlated with the QST factor score. Clusters in hot colours are regions with positive loadings, and clusters in cold colours are regions with negative loadings. (C) The mean absolute CBF values extracted from the unified network within regions with positive, negative loadings and the remaining regions outside of the unified component, in knee pain participants and controls (plotted with standard error of the mean). (D) Mean CBF of the regions with positive loadings of component 12 (red clusters in B) correlated with the QST factor score. CBF, cerebral blood flow; QST, quantitative sensory testing.

reported in O'Muircheartaigh et al. with both displaying increased CBF of the thalamus. It is tempting to speculate that persistent thalamic activation may be a key process in driving pain chronification. In fact, thalamic volume changes have been observed in participants with chronic hip OA pain; moreover, this effect is normalized following successful arthroplasty intervention.<sup>18</sup> In our data, the right dorsomedial nucleus was specifically observed to be hyperperfused in the chronic knee pain group and this was seen across the unified components map as well as the component that showed a correlation with QST measures. This nucleus is part of the medial pain pathway that is responsible for the affective-motivational elements of pain perception and, moreover, has extensive connections with the cortex including somatosensory and limbic regions,<sup>1</sup> akin to those regions we observed to be hypoperfused in participants with chronic knee pain. The association between one of the discriminating components with the QST score aligns well with the notion that aberrancies within this network are more pronounced in those who are more centrally sensitized to pain. The continuous nociceptive barrage may result in a sensitized state of the thalamic circuitry that links to numerous areas of higher-order cognitive processes.<sup>1</sup> This cascading effect of the overactive thalamus may explain the lack of deactivation of posterior DMN regions in our chronic knee pain participants and perhaps extend to affect other sensory (visual) regions. The reverse pattern observed in the aforementioned acute postsurgical pain study<sup>33</sup> may be a demonstration of the normal function of this thalamic circuitry to effectively upregulate and downregulate salience and default mode regions, respectively, during an acute pain experience. By contrast, in chronic knee pain, continuous peripheral input may have resulted in a breakdown of this system leading to dysfunctional bottom-up processes and an abnormal interaction between salience and default mode networks. This

constant peripheral pain drive has previously been proposed to maintain sensitization of central pain pathways in MSK pain.<sup>17</sup>

Kucyi et al.<sup>25</sup> found that spontaneous mind wandering away from pain resulted in increases in DMN activity with greater salience network activity when attending to pain. This is consistent with the present findings of increased and decreased perfusion in the DMN and salience regions, respectively, in chronic knee pain participants who had lower sensitivity to pain. The higher activity of the posterior cingulate, precuneus and cuneus regions in less sensitized participants may allow these participants being better able to assess and appropriately orient attention toward and/or away from pain. We speculate that the greater effectiveness of this system may have enabled participants with chronic knee pain to become better adapted to cope with frequent nociceptive input and thus preventing central sensitization. The deactivation of regions such as the insula and anterior cingulate cortex may be reflective of hypoarousal and a lesser ability for interoception. There may be a complex interplay between the salience and default mode networks that result in an impaired capacity to effectively disengage their attention to pain. Although purely speculative, this difference in the ability to attend to or disengage from pain may determine the reorganisation of one's brain circuitry during the chronification and central sensitization process.

#### 4.2. Changes in the periaqueductal gray in chronic knee pain

It is, however, surprising that the PAG was not evident as a pain-relevant region in our cohort given previous reports of PAG changes in chronic pain<sup>10,19,21,25,40</sup> and its well-documented involvement in the antinociceptive system for inhibition of pain.<sup>5,29,34</sup> One might expect this region to robustly differentiate chronic knee pain participants from pain-free controls and

**Table 4****Cluster maxima of the unified of components that significantly classified knee pain participants from controls.**

Region	Cluster size (voxels)*	MNI coordinates			Z value
		X	Y	Z	
Hyperperfusion in chronic knee pain					
Lateral occipital, cuneus, precuneus, and posterior cingulate cortex	3320	−14	−84	40	4.03
Cerebellum	1907	8	−88	−32	3.84
Fusiform gyrus and inferior temporal gyrus	349	−42	−26	−22	2.99
Inferior temporal gyrus and lateral occipital cortex	252	54	−62	−12	2.85
Lingual gyrus and parahippocampal gyrus	131	−14	−42	−10	2.4
Lateral occipital cortex	124	−40	−76	18	3.11
Cerebellum	83	−26	−52	−56	3.1
Cerebellum	52	−6	−50	−60	2.86
Brain stem	46	−4	−44	−62	3.86
Temporal pole	43	−48	22	−24	2.8
Thalamus	41	4	−18	10	2.4
Inferior temporal gyrus	39	48	−6	−46	2.71
Lingual gyrus	38	16	−68	−2	2.54
Parahippocampal gyrus	36	−26	−22	−20	2.49
Frontal pole	28	−12	66	24	2.18
Lateral occipital cortex and fusiform gyrus	23	−44	−74	−16	2.53
Frontal pole	22	−6	70	8	2.26
Parahippocampal gyrus and fusiform gyrus	21	26	−10	−38	2.52
Caudate	20	−16	−10	24	2.49
Hypoperfusion in chronic knee pain					
Supramarginal gyrus, postcentral gyrus, and parietal operculum	1339	−58	−20	28	3.42
Frontal pole	1004	30	54	10	3.52
Cerebellum	633	28	−38	−50	4.68
Heschl's gyrus, planum polare, and insula	537	−44	−16	6	3.35
Anterior cingulate cortex	533	−2	42	10	3.07
Orbitofrontal cortex	441	0	30	−20	3.23
Orbitofrontal cortex and anterior insula	392	36	24	−8	3.84
Opercular cortex	241	42	−12	18	2.89
Cerebellum	219	−48	−58	−50	3.81
Postcentral gyrus and supramarginal gyrus	208	52	−26	40	2.89
Frontal pole	185	−32	52	6	2.97
Midcingulate gyrus	121	0	−4	36	2.5
Orbitofrontal cortex, inferior frontal gyrus, and anterior insula	110	−34	30	−2	2.89
Postcentral gyrus and supramarginal gyrus	101	38	−32	42	3.14
Precentral gyrus and inferior frontal gyrus	89	54	10	32	3.23
Lateral occipital cortex and angular gyrus	74	42	−60	56	2.83
Lateral occipital cortex and superior parietal cortex	67	−24	−58	68	2.37
Middle frontal gyrus and inferior frontal gyrus	63	42	22	30	3.14
Anterior cingulate cortex	62	12	40	14	2.62
Cerebellum	54	−28	−82	−44	2.56
Inferior frontal gyrus and precentral gyrus	51	56	10	12	3.02
Inferior temporal gyrus and middle temporal gyrus	35	−56	−10	−32	2.6
Superior temporal gyrus, planum temporale, and Heschl's gyrus	34	−58	−4	−2	2.57
Superior frontal gyrus	34	12	10	62	2.93
Orbitofrontal cortex	31	−20	30	−22	2.69
Middle frontal gyrus	30	40	10	48	2.82
Planum temporale and insula	26	−46	2	−12	2.43
Frontal pole	23	−24	44	20	2.43
Orbitofrontal cortex	22	22	12	−16	2.38
Angular gyrus and supramarginal gyrus	22	−50	−52	28	2.52
Superior frontal gyrus and supplementary motor cortex	21	10	10	58	2.91

\*Only clusters &gt;20 voxels in size are listed.

furthermore be related to sensitization of central pain mechanisms, particularly if our theory above regarding the attending toward/away from pain is true. However, the spatial resolution that is feasible with ASL does not allow for the segregation of the subcomponents of the PAG, and therefore, the signal measured from the PAG will be an average across both the ascending and descending pain pathways, which are known to have distinct connections and mechanisms underlying the pain experience.<sup>29</sup>

Furthermore, small clusters are less likely to be detected using a PCA approach due to the thresholds applied for explained variance. A post hoc exploratory analysis of the PAG in our data set revealed that, similarly to a previous report,<sup>21</sup> there is indeed increased perfusion in participants with chronic knee pain (supplementary Figure 1, available at <http://links.lww.com/PAIN/A966>), suggesting that although there are PAG alterations in chronic knee pain, the PAG perfusion pattern may not contribute to

the major CBF networks derived through the PCA approach across the full data set. It would be of interest to further investigate in the same individuals whether there is a link between CBF increases of the PAG (as seen in the current study) and altered connectivity of the PAG with default mode regions (as seen in ref. 25).

### 4.3. Negative affect in chronic knee pain

The lack of association between the affective score and CBF is not unexpected. Although our patient cohort scored significantly higher for affective elements, the majority (>93%) scored below cut offs indicative of severe depression and/or anxiety. Therefore, the present data set may lack the variation in affective features to be able to effectively test our hypothesis. We also suggest that the PCA approach be applied to a chronic pain cohort (ideally with high variation of affective measures) to identify components that differentiate participants with high and low negative affective features to better deconstruct the effect of psychological aspects contributing to chronic pain. In addition, the natural next step is to validate this model using an independent data set to test the predictive confidence and generalizability.

### 4.4. Limitations

A limitation of our study is that a proportion of our chronic pain participants had taken opioid medication and/or antidepressants, which could have affected CBF especially within the salience and default mode regions. However, comparison of the mean CBF values of both the positive and negative loadings of the unified component between those on opioid or antidepressant medication and those who were not showed no significant difference (see supplementary materials for detailed results, available at <http://links.lww.com/PAIN/A966>). Moreover, visual inspection of the correlation between the QST factor score and both the component 12 network score and the mean CBF of component 12 positive loadings did not show a systematic pattern to suggest there was a strong impact of medication on the current findings (colour-coded correlation plot of Fig. 1D is available in the supplementary materials, available at <http://links.lww.com/PAIN/A966>). Further limitations are the smaller number of controls than pain participants and the lack of power and sample size calculation, which is due to the novelty of the approach in chronic pain. Nevertheless, this data set is larger than those usually recommended for ASL studies<sup>7,11,20,21,24,32,39</sup> and in line with published multivariate pattern analysis studies in psychiatric conditions.<sup>23</sup> Also, to maintain maximum power in the given data set, we refrained from sample splitting and out of sample validation. Generalizability of our reported chronic pain-related CBF pattern will hence need to be validated in the future. This is an obvious avenue of work in a large chronic pain data set to be recruited in the near future.

## 5. Conclusions

This study successfully delineated participants with chronic knee pain from controls using a PCA approach on CBF data, and the discrimination was related to the degree of pain sensitization as measured through comprehensive QST methods. The patterns of CBF alterations indicate greater blood flow changes in primarily the salience and default mode network regions commonly implicated in chronic pain, and these were further heightened in those with greater central sensitization. This pattern was unrelated to the pain severity on the day and largely opposite to the reported CBF signature of acute postsurgical pain further pointing to a neuroplastic and also a potentially non-nociceptive

origin. We demonstrate that task-free CBF assessment contains important covariance features that may signify the neural mechanisms of pain chronification and pain sensitization.

## Conflict of interest statement

The authors have no conflicts of interest to declare.

## Acknowledgements

The authors are also indebted to colleagues who enabled recruitment (Nadia Frowd, Dr Bonnie Millar, Marya Habib, Louise Borg and Debbie Wilson), refactored the code for PCA analysis (Dr S Pszczolkowski), and scanned participants (Andrew Cooper). This work was supported by Versus Arthritis [grant 20777]; YX was supported by Parkinson's UK [grant J-1204] and Michael J Fox Foundation [grant 11473]. AT was supported by the Haydn Green Foundation and the University of Nottingham VC scholarship. Center for Neuroplasticity and Pain (CNAP) is supported by the Danish National Research Foundation (DNRF121). All authors declare no conflicts of interest.

## Appendix A. Supplemental digital content

Supplemental digital content associated with this article can be found online at <http://links.lww.com/PAIN/A966>.

## Article history:

Received 8 September 2019

Received in revised form 31 January 2020

Accepted 4 February 2020

Available online 14 February 2020

## References

- [1] Ab Aziz CB, Ahmad AH. The role of the thalamus in modulating pain. *Malays J Med Sci* 2006;13:11–18.
- [2] Alsop DC, Detre JA, Golay X, Gunther M, Hendrikse J, Hernandez-Garcia L, Lu HZ, MacIntosh BJ, Parkes LM, Smits M, van Osch MJP, Wang DJJ, Wong EC, Zaharchuk G. Recommended implementation of arterial spin-labeled perfusion MRI for clinical applications: a consensus of the ISMRM perfusion study group and the European Consortium for ASL in Dementia. *Magnet Reson Med* 2015;73:102–16.
- [3] Baliki MN, Geha PY, Apkarian AV, Chialvo DR. Beyond feeling: chronic pain hurts the brain, disrupting the default-mode network dynamics. *J Neurosci* 2008;28:1398–403.
- [4] Baliki MN, Mansour AR, Baria AT, Apkarian AV. Functional reorganization of the default mode network across chronic pain conditions. *PLoS One* 2014;9:e106133.
- [5] Basbaum AI, Fields HL. Endogenous pain control mechanisms: review and hypothesis. *Ann Neurol* 1978;4:451–62.
- [6] Beck A, Steer R, Brown G. Manual for the Beck depression inventory-II. San Antonio: Psychological Corporation, 1996.
- [7] Boissoneault J, Letzen J, Lai S, Robinson ME, Staud R. Static and dynamic functional connectivity in patients with chronic fatigue syndrome: use of arterial spin labelling fMRI. *Clin Physiol Funct Imag* 2018;38:128–37.
- [8] Breivik H, Collett B, Ventafridda V, Cohen R, Gallacher D. Survey of chronic pain in Europe: prevalence, impact on daily life, and treatment. *Eur J pain* 2006;10:287–333.
- [9] Ceko M, Shir Y, Ouellet JA, Ware MA, Stone LS, Seminowicz DA. Partial recovery of abnormal insula and dorsolateral prefrontal connectivity to cognitive networks in chronic low back pain after treatment. *Hum Brain Mapp* 2015;36:2075–92.
- [10] Cheriyan J, Sheets PL. Altered excitability and local connectivity of mPFC-PAG neurons in a mouse model of neuropathic pain. *J Neurosci* 2018;38:4829–39.
- [11] Cottam WJ, Condon L, Alshuft H, Reckziegel D, Auer DP. Associations of limbic-affective brain activity and severity of ongoing chronic arthritis pain are explained by trait anxiety. *NeuroImage Clin* 2016;12:269–76.



- [12] Dahlhamer J, Lucas J, Zelaya C, Nahin R, Mackey S, DeBar L, Kerns R, Von Korff M, Porter L, Helmick C. Prevalence of chronic pain and high-impact chronic pain among adults—United States, 2016. *MMWR Morbid Mortal Wkly Rep* 2018;67:1001–6.
- [13] Dai W, Garcia D, de Bazelaire C, Alsop DC. Continuous flow-driven inversion for arterial spin labeling using pulsed radio frequency and gradient fields. *Magn Reson Med* 2008;60:1488–97.
- [14] Fayaz A, Croft P, Langford RM, Donaldson LJ, Jones GT. Prevalence of chronic pain in the UK: a systematic review and meta-analysis of population studies. *BMJ Open* 2016;6:e010364.
- [15] Fernandes GS, Sarmanova A, Warner S, Harvey H, Akin-Akinyosoye K, Richardson H, Frowd N, Marshall L, Stocks J, Hall M, Valdes AM, Walsh D, Zhang W, Doherty M. Knee pain and related health in the community study (KPIC): a cohort study protocol. *BMC Musculoskelet Disord* 2017;18:404.
- [16] Fernandes GS, Valdes AM, Walsh DA, Zhang W, Doherty M. Neuropathic-like knee pain and associated risk factors: a cross-sectional study in a UK community sample. *Arthritis Res Ther* 2018;20:215.
- [17] Graven-Nielsen T, Arendt-Nielsen L. Assessment of mechanisms in localized and widespread musculoskeletal pain. *Nat Rev Rheumatol* 2010;6:599–606.
- [18] Gwilym SE, Filippini N, Douaud G, Carr AJ, Tracey I. Thalamic atrophy associated with painful osteoarthritis of the hip is reversible after arthroplasty: A longitudinal voxel-based morphometric study. *Arthritis Rheum* 2010;62:2930–40.
- [19] Gwilym SE, Keltner JR, Warnaby CE, Carr AJ, Chizh B, Chessell I, Tracey I. Psychophysical and functional imaging evidence supporting the presence of central sensitization in a cohort of osteoarthritis patients. *Arthritis Rheum* 2009;61:1226–34.
- [20] Hodkinson DJ, Veggeberg R, Wilcox SL, Scrivani S, Burstein R, Becerra L, Borsook D. Primary somatosensory cortices contain altered patterns of regional cerebral blood flow in the interictal phase of migraine. *PLoS One* 2015;10:e0137971.
- [21] Howard MA, Sanders D, Krause K, O'Muircheartaigh J, Fotopoulou A, Zelaya F, Thacker M, Massat N, Huggins JP, Vennart W, Choy E, Daniels M, Williams SC. Alterations in resting-state regional cerebral blood flow demonstrate ongoing pain in osteoarthritis: an arterial spin-labeled magnetic resonance imaging study. *Arthritis Rheum* 2012;64:3936–46.
- [22] Jenkinson M, Beckmann CF, Behrens TE, Woolrich MW, Smith SM. FSL. *Neuroimage* 2012;62:782–90.
- [23] Kambitz J, Cabral C, Sacchet MD, Gotlib IH, Zahn R, Serpa MH, Walter M, Falkai P, Koutsouleris N. Detecting neuroimaging biomarkers for depression: a meta-analysis of multivariate pattern recognition studies. *Biol Psychiatry* 2017;82:330–8.
- [24] Keszthelyi D, Aziz Q, Ruffle JK, O'Daly O, Sanders D, Krause K, Williams SCR, Howard MA. Delineation between different components of chronic pain using dimension reduction—an ASL fMRI study in hand osteoarthritis. *Eur J Pain* 2018;22:1245–54.
- [25] Kucyi A, Salomons TV, Davis KD. Mind wandering away from pain dynamically engages antinociceptive and default mode brain networks. *Proc Natl Acad Sci U S A* 2013;110:18692–7.
- [26] Kulkarni B, Bentley DE, Elliott R, Julyan PJ, Boger E, Watson A, Boyle Y, El-Deredy W, Jones AKP. Arthritic pain is processed in brain areas concerned with emotions and fear. *Arthritis Rheum* 2007;56:1345–54.
- [27] Liang X, Zou Q, He Y, Yang Y. Coupling of functional connectivity and regional cerebral blood flow reveals a physiological basis for network hubs of the human brain. *Proc Natl Acad Sci U S A* 2013;110:1929–34.
- [28] Lincoln N, Moreton B, Turner K, Walsh D. The measurement of psychological constructs in people with osteoarthritis of the knee: a psychometric evaluation. *Disabil Rehabil* 2017;39:372–84.
- [29] Linnman C, Moulton EA, Barnettler G, Becerra L, Borsook D. Neuroimaging of the periaqueductal gray: state of the field. *Neuroimage* 2012;60:505–22.
- [30] Loggia ML, Kim J, Gollub RL, Vangel MG, Kirsch I, Kong J, Wasan AD, Napadow V. Default mode network connectivity encodes clinical pain: an arterial spin labeling study. *PAIN* 2013;154:24–33.
- [31] Melzer TR, Watts R, MacAskill MR, Pearson JF, Rueger S, Pitcher TL, Livingston L, Graham C, Keenan R, Shankaranarayanan A, Alsop DC, Dalrymple-Alford JC, Anderson TJ. Arterial spin labelling reveals an abnormal cerebral perfusion pattern in Parkinson's disease. *Brain* 2011;134:845–55.
- [32] Murphy K, Harris AD, Diukova A, Evans CJ, Lythgoe DJ, Zelaya F, Wise RG. Pulsed arterial spin labeling perfusion imaging at 3 T: estimating the number of subjects required in common designs of clinical trials. *Magn Reson Imag* 2011;29:1382–9.
- [33] O'Muircheartaigh J, Marquand A, Hodkinson DJ, Krause K, Khawaja N, Renton TF, Huggins JP, Vennart W, Williams SC, Howard MA. Multivariate decoding of cerebral blood flow measures in a clinical model of on-going postsurgical pain. *Hum Brain Mapp* 2015;36:633–42.
- [34] Ossipov MH, Morimura K, Porreca F. Descending pain modulation and chronicification of pain. *Curr Opin Support Palliat Care* 2014;8:143–51.
- [35] Petersen KK, Arendt-Nielsen L, Finocchietti S, Hirata RP, Simonsen O, Laursen MB, Graven-Nielsen T. Age interactions on pain sensitization in patients with severe knee osteoarthritis and controls. *Clin J Pain* 2017;33:1081–7.
- [36] Phillips CJ. The cost and burden of chronic pain. *Rev Pain* 2009;3:2–5.
- [37] Rathleff MS, Petersen KK, Arendt-Nielsen L, Thorborg K, Graven-Nielsen T. Impaired conditioned pain modulation in young female adults with long-standing patellofemoral pain: a single blinded cross-sectional study. *Pain Med* 2016;17:980–8.
- [38] Schnack HG, Kahn RS. Detecting neuroimaging biomarkers for psychiatric disorders: sample size matters. *Front Psychiatry* 2016;7:50.
- [39] Segerdahl AR, Mezue M, Okell TW, Farrar JT, Tracey I. The dorsal posterior insula subserves a fundamental role in human pain. *Nat Neurosci* 2015;18:499–500.
- [40] Soni A, Wanigasekera V, Mezue M, Cooper C, Javaid MK, Price AJ, Tracey I. Central sensitization in knee osteoarthritis: relating presurgical brainstem neuroimaging and PainDETECT-based patient stratification to arthroplasty outcome. *Arthritis Rheumatol* 2019;71:550–60.
- [41] Spetsieris PG, Ma Y, Dhawan V, Eidelberg D. Differential diagnosis of parkinsonian syndromes using PCA-based functional imaging features. *Neuroimage* 2009;45:1241–52.
- [42] Spielberger C, Gorsuch R, Lushene R, Vagg PR, Jacobs GA. *Manual for the State-Trait Anxiety Inventory*. Palo Alto: Consulting Psychologists Press, 1983.
- [43] Sullivan MJL, Bishop SR, Pivik J. The pain catastrophizing scale: development and validation. *Psychol Assess* 1995;7:524–32.
- [44] Vaegter HB, Graven-Nielsen T. Pain modulatory phenotypes differentiate subgroups with different clinical and experimental pain sensitivity. *PAIN* 2016;157:1480–8.
- [45] Wager TD, Atlas LY, Lindquist MA, Roy M, Woo CW, Kross E. An fMRI-based neurologic signature of physical pain. *N Engl J Med* 2013;368:1388–97.
- [46] Wartolowska KA, Bulte DP, Chappell MA, Jenkinson M, Okell TW, Webster M, Carr AJ. Using arterial spin labelling to investigate spontaneous and evoked ongoing musculoskeletal pain. *bioRxiv* 2018:163196.
- [47] Wasan AD, Loggia ML, Chen LQ, Napadow V, Kong J, Gollub RL. Neural correlates of chronic low back pain measured by arterial spin labeling. *Anesthesiology* 2011;115:364–74.
- [48] Zaharchuk G, Straka M, Marks MP, Albers GW, Moseley ME, Bammer R. Combined arterial spin label and dynamic susceptibility contrast measurement of cerebral blood flow. *Magnet Reson Med* 2010;63:1548–56.